AIAA 2013-2158

Numerical and experimental analysis of flow-acoustic interactions in an industrial gate valve

Romain Lacombe*, Philippe Lafon †, Frédéric Daude *and Fabien Crouzet *
EDF R&D, LaMSID UMR EDF-CEA-CNRS 8193, Clamart, France

Christophe Bailly‡
LMFA UMR CNRS 5509, Ecully, France

Samir Ziada§
McMaster University, Hamilton, Ontario, Canada

I. Introduction

Strong tonal noise can be found on the main steam lines of power plants. The source of noise was identified to be located at the gate valves present on the steam lines. Analysis of on-site measurements showed that the source of noise was due to the cavity that forms the valve seat at the bottom of the valve body. The valve in its open position is then composed of this bottom cavity over which an unstable shear layer develops but also of the top cavity where the gate is stored in open position. The valve is of course also connected to the pipe. All these elements are good candidates for flow-acoustic phenomena. The development of the shear layer over the cavity gives rise to self-sustained flow oscillations and noise radiation. The vortices convected in the shear layer which develops from the upstream corner of the cavity interact with the downstream corner of the cavity. A pressure disturbance is then generated and acts as a feedback loop on the separation point at the upstream corner. Due to the phase relationship between the generation of the disturbance downstream and its influence upstream, this pressure feedback selection amplifies the shear layer and preferred modes of oscillation are then produced. It is also well known that at low Mach number these pressure oscillations in the cavity remain weak. However, in ducted configurations, powerful tones can be generated even at low Mach number when pressure oscillations in the shear layer couple with the acoustical response of the duct.

In order to study these phenomena in configurations close to the industrial ones, both numerical and experimental approaches are carried out. A high-order numerical code has been developed in order to capture aeroacoustic interactions in turbulent flows. An experimental test rig has been built in order to study aeroacoustic phenomena in small scale models of control flow devices present on steam pipes of power plants. A vacuum pump is used instead of a ventilator for creating the flow through the test rig in order to study high pressure loss devices.

The present paper aims at handling the flow-acoustic phenomena in the case of a fully 3D geometry of the gate valve. Both numerical and experimental investigation methods are used. In the second section of the paper, industrial problem and previous study are recalled. In the third section, the small scale model that is used for both numerical and experimental investigations is presented. In the fourth section, the numerical methods used in this paper are presented. In the fifth section, the experimental device and the measurements techniques are presented. In the sixth section, results of the acoustic modal analysis of the valve are analysed. In the seventh section, results of the flow-acoustic analysis of phenomena in the valve are analysed.

*Research Engineer
†Senior Research Engineer, AIAA Member
‡Professor, AIAA Member
§Professor

II. Tonal noise generation in an industrial gate valve

When mounted in a steam pipe of a power plant, gate valves are used as isolation valve if an incident occurs on the piping system. Figure 1 gives an overview of the gate valve location in a simple sketch of a power plant. The valve is mainly composed of a gate and of a seat. When the valve is open, the gate is located in the top part of the valve body, as illustrated in Figure 1. When the valve is closed, the gate slides along rails and makes contact with the seat, creating then a sealing surface.

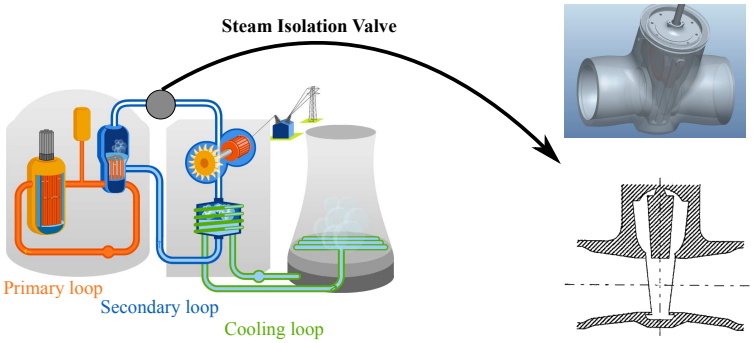

Figure 1. Design of the steam isolation gate valve and its location in a power plant.

When the valve is open, the bottom part of the seat forms a shallow cavity above which a shear layer develops. The vortices convected in the shear layer which develops from the upstream corner of the cavity interact with the downstream corner of the cavity. A pressure disturbance is then generated and acts as a feedback loop on the separation point at the upstream corner. Due to the phase relationship between the generation of the disturbance downstream and its influence upstream, this pressure feedback selection amplifies the shear layer and preferred modes of oscillation are then produced. These oscillation modes are the Shear Layer Modes and are expressed by the semi-empirical Rossiter's formula.[14,15] It is also well known that at low Mach number these pressure oscillations in the cavity remain weak. However, in ducted configurations, powerful tones can be generated even at low Mach number when pressure oscillations in the shear layer couple with the acoustical response of the duct ie when Shear Layer Modes lock in with Acoustic Duct Modes. The problem of cavity noise in confined flow has been extensively studied by Aly and Ziada[1–3] especially through the analysis of trapped modes.

The industrial problem related to gate valve noise generation is well known and has been studied in previous papers.[11,12,17] More recent studies[7,8] have dealt with a quasi 3-D configuration representing a ducted cavity. This configuration was a simplified model of the fully 3D case, the goal being to show the ability of numerical simulations to well capture the flow-acoustic coupling. As a reminder, some results are displayed in Figure 2. The coupling between the shear layer modes and the duct acoustic modes is well retrieved and more particularly, Figure 2 represents the lock-in between the second shear layer mode characterized by the presence of two vortices in the shear layer, and the first acoustic duct mode.

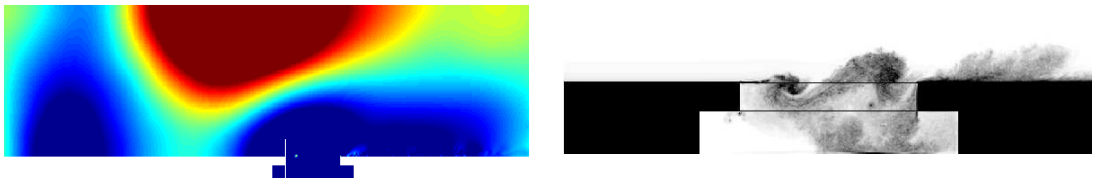

Figure 2. 2-D ducted cavity with an inlet flow at $M_\infty = 0.18$; left view: pressure fluctuations in the duct (< 100 Pa), right view: spanwise average vorticity modulus in the cavity.

III. Small scale model

The first step of the study was to define a small scale model of the real valve in order to be used for both computations and experiments. Indeed in this industrial configuration, the working fluid is the steam and the Mach and Reynolds numbers at the smallest section of the valve are 0.15 and 8×10^7. For the present study, we used air as working fluid and the reachable flow rate is limited by the test rig configuration. So a small scale model is used. This model keeps the same dimensions ratio and is scaled in order to have a flow

Mach number ranging between 0.1 and 0.2 at the smallest section of the valve. This Mach number range includes the Mach number reached in the industrial configuration. The present scaling leads to a model 5 times smaller than the real geometry. The scaling on Mach number is appropriate, as it preserves both the acoustic scaling, *i.e.* a constant Helmholtz number, and the source scaling, *i.e.* a constant Strouhal number. The Reynolds number in the small scale model is around 4×10^5. The consequence of operating at a lower Reynolds number than for the industrial configuration is considered to be negligible on the flow induced pulsations, as the flow is turbulent in the model and the flow profile above the cavity is typical of the one found in the industrial flow conditions.

Figure 3 depicts the experimental small scale model with its probe supports. The discretized computational domain used for the simulations corresponds to the inner domain of this model. The inlet and outlet pipes diameter is 132.7 mm. The smallest pipe diameter, just upstream of the valve seat, is 94 mm. The gap between the two edges of the bottom cavity is 33 mm. The model represents the valve in its open position. Six 1/4 inches microphones can be mounted on the experimental model, five supports are visible in Figure 3, the last one being at the top cavity of the valve. The bottom cavity is made removable so that different designs could be tested.

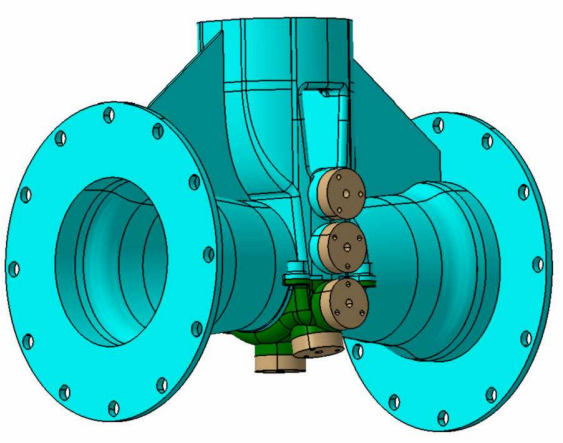

Figure 3. Representation of the experimental small scale model with the probe supports and the removable cavity.

IV. Numerical methods

The study of the aeroacoustic interaction in the gate valve is done with numerical simulations and experimental measurements. To deal with the numerics, the high-order parallel structured multiblock compressible solver *Code_Safari*[6] has been developed at EDF.

LES solver

The set of equations are the compressible 3-D Navier-Stokes equations, written in conservative form after application of a general time-invariant curvilinear coordinates transformation from physical space to computational space. This transformation $(x, y, z) \rightarrow (\xi, \eta, \zeta)$ yields to a new expression for the Navier-Stokes equations:

$$\frac{\partial}{\partial t}\left(\frac{\mathbf{Q}}{J}\right) + \frac{\partial \mathbf{E}}{\partial \xi} + \frac{\partial \mathbf{F}}{\partial \eta} + \frac{\partial \mathbf{G}}{\partial \zeta} = 0,$$

where J is the Jacobian of the geometric transformation. The unknown vector writes $\mathbf{Q} = (\rho, \rho u, \rho v, \rho w, \rho e_t)^T$, where ρ designates the density, u, v, w the Cartesian velocity components and ρe_t the total energy. The latter is calculated for a perfect gas such as $\rho e_t = p/(\gamma - 1) + \frac{1}{2}\rho(u^2 + v^2 + w^2)$ with p the pressure. The flux vectors $\mathbf{E}$, $\mathbf{F}$, $\mathbf{G}$ contain the inviscid and the viscous terms. Their expressions as well as the metric identities for the grid transformation can be found in the literature.[13,19]

For interior points of the computational domain, the fluxes and the velocity derivatives for the viscous terms are discretized by standart 7-points or optimized 11-points centered finite difference schemes.[4] An explicit fourth-order low-storage Runge-Kutta scheme advances the solution in time. The CFL number is

Figure 4. Gate valve model meshed with 38 overset grids. Some elementary grids are depicted.

0.9 and the time step Δt is updated every iteration during the transient phase. Appropriate 7-points or 11-points explicit low pass filters remove grid-to-grid oscillations, not resolved by centered finite difference schemes.[4] At the same time, the filters properly remove non-resolved turbulent structures and so act like a subgrid scale model. This method referred as LES-RF has been successfully applied in the literature.[5,9]

The finite difference schemes are limited to structured grids. In order to treat more complex geometries, a high-order overset capability has been implemented in the code. In this approach, the computational domain is subdivided into overlapping structured component grids. The governing equations are solved on each component grid separately and the communication between grids is achieved through interpolations. For grid generation *Ogen*, the grid assembler module of the freely available library *Overture*[10] developed at the Lawrence Livermore National Laboratory, has been interfaced with the solver. For communication between grid boundaries that do not coincide, high-order interpolation is used. Lagrangian polynomials has been found to be best suited in terms of precision, execution time and implementation aspects for the high-order overset grid approach.[16] Various tests have shown that at least eighth-order polynomials have to be used in order to make the interpolation error negligible when using the 11-points scheme and fourth-order polynomials when using the 7-points scheme.

The standard Message Passing Interface (MPI) library routines have been used for code parallelization and, for load balancing purpose, each component grid is subdivided evenly N times in each direction and can be computed by $N_{\text{procs}} = N_{\xi,\text{procs}} \times N_{\eta,\text{procs}} \times N_{\zeta,\text{procs}}$..

Boundary conditions

At the inlet and the outlet, non-reflective boundary conditions issued from[18] are applied. They correspond to far field acoustic boundary conditions.

At the inlet, a velocity flow profile is imposed. As no experimental results were yet available for the simulation presented in this paper, a turbulent pipe flow profile was imposed at the inlet. The mean flow velocity is 50 m/s. As the flow profile just upstream of the bottom cavity of the gate does not fit with the experiments, direct comparison between the results cannot be achieved, this velocity profile playing a crucial role in the characteristics of the tonal noise generation. So only qualitative comparison will be done here. Future simulations, fitted to the experiments, will come later.

Linear acoustic solver

In order to help the acoustic analysis of the flow-acoustic interaction results obtained by LES or by experimental approaches, a linear acoustic solver has heen developed in *Code_Safari*. This solver is based on the linearized Euler equations. If the unsteady inviscid flow is described as the sum of a mean component, and of a small amplitude disturbance, then Euler equations becomes linear. If it is also assumed that the unsteady

disturbances are harmonic in time with frequency ω, the small disturbances (linearized Euler equations) writes :

$$j\omega\mathbf{u} + \frac{\partial(\mathbf{Au})}{\partial x} + \frac{\partial(\mathbf{Bu})}{\partial y} + \frac{\partial(\mathbf{Cu})}{\partial z} + \mathbf{H} = \mathbf{S},$$

where $\mathbf{u}$ is the complex amplitude of the small disturbances. $\mathbf{A}$, $\mathbf{B}$, $\mathbf{C}$ are matrices based on mean flow variables. $\mathbf{H}$ is a matrix based on $\mathbf{u}$ and mean flow variables. The vector $\mathbf{S}$ allows to impose acoustic sources. A common approach for solving this equation is to add a pseudo-time term. Then the numerical solution can be marched in time and when reaching steady state, the pseudo-time term becomes zero and the solution of the linearized equations is obtained. For the spatial fluxes, the same discretization techniques as for the LES solver are used. Non-reflective boundary conditions issued from[18] are applied at the inlet and at the outlet.

Overset grid for the valve

As introduced above, an overset-grid strategy is used to deal with the complex 3D geometry. In the present case, we started from a CAD model of the small scale model of the valve, similarly to the experiments. Then, several surface grids were built on the inner walls of the valve model. Each of these grids were then extruded in the normal direction to the walls in order to create volume grids. To fill the inner volume of the geometry, core grids were then added. All these grids always overlaps on their neighbours. At the end, the interpolation of each grid with its neighbours was calculated, giving the final computational domain on which LES can be done with *Code_Safari*. The Figure 4 illustrates the meshing methodology. It presents the whole computational domain and shows some of elementary grids making up the domain. These elementary grids are presented as surface grids, without the extrusion in the normal direction which is applied to generate the volume grid.

The final computational domain is composed of 38 grids, with a total of 78 million points and 9 million interpolation points. The smallest grid elements are situated at the wall in the seat and gate regions. Their size is about 3×10^{-4} m. In the core region, the discretization size is coarser, such that in the centre of the pipe, the grid elements are four times bigger than at the walls. Moreover, upstream and downstream of the seat region, the discretization is coarser and stretched in the inlet and outlet direction. Different elementary grids overlap to do an efficient coarsing of the discretization. The discretization jump between two overlapping grids is however kept below a factor of two to keep accurate interpolation between them. Just before the outlet, two grids, one for the wall and one for the core, play the role of sponge zone. They have the coarsest discretization size, the meshes are stretched in the outlet direction and an artificial viscosity is added in this direction. The role of these grids is to dissipate all the vortical structures before the outlet boundary conditions.

V. Experimental approach

Description of the test rig

The test rig, depicted in Figure 5, is composed of a vacuum pump suction the air of the laboratory inside pipes. Between the pump and the test section, a tunable sonic nozzle is mounted in order to create subsonic stable flow. This sonic nozzle has been calibrated with Pitot measurement. The test section is composed of two 3 meters long pipes, the small scale model being mounted in-between. At the inlet a contraction nozzle is mounted to take the flow from the laboratory room to the test section.

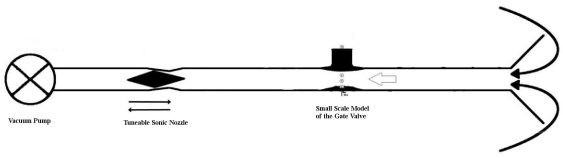

Figure 5. Scheme of the test rig.

Two measurements have been done on the small scale model, first a modal analysis without flow then acoustic measurements with flow. Both are described in the next two subsections.

Modal analysis without flow

In order to characterize the valve eigenfrequencies, a modal analysis has been done without flow. Six measurements were done, each one consisting of exciting the valve from one of each orifice used as probe support. The analysis is done frequency by frequency, as the excitation consists in pure sine, from 200 Hz to 4000 Hz with a 10 Hz step. For each excitation by one orifice, we have measured the transfer functions between a reference microphone located at the valve inlet and the five microphones mounted on the probe supports, *c.f.* Figure 3. These measurements gave the valve eigenfrequencies as well as the phase relation between acoustic pressures at the six microphone locations.

Flow-excited resonance measurements

The second step in the experimental approach, is to measured the tonal noise when flow-acoustic coupling exists in the valve. Acoustic pressures were measured at the six locations of the microphone in the valve. Pressure spectra and transfer function between microphones were stored during each experiment at a specific flow velocity. The experiments were done for a mean flow velocity above the gate valve cavity ranging from around 50 m/s to 125 m/s. This corresponds to a Mach number ranging from 0.14 to 0.36.

Hot wire measurements just upstream of the gate valve cavity can be done on the test rig. This hot wire measurements are not presented here, as they are currently underway. They will be used for future analysis and also as input data for the future flow simulation. Thus, simulations presented in this paper do not use an experimental inlet flow profile.

VI. Acoustic modal analysis without flow

As indicated previously, a modal analysis of the gate valve without flow has been done. The goal is to identify the eigenfrequencies of the geometry and to compare them with the whistling frequencies observed when a subsonic flow generates self-sustained oscillations.

In a first step, this modal analysis was done experimentally. The valve inner domain was excited with a loudspeaker mounted on each orifice of the valve, *i.e.* from each of the six probe supports. Using sine excitations ranging from 200 Hz to 4000 Hz, with a frequency step of 10 Hz, the absolute value and the phase of the transfer functions between a reference microphone located at the inlet of the valve and the five microphones mounted in the five remaining probe supports were measured.

Figure 6 present the magnitude and phase of the transfer functions measured when the excitation is from the second orifice in the bottom cavity, *c.f.* Figure 3. On the magnitude plot, the acoustic modes are thus identified at the peak locations.

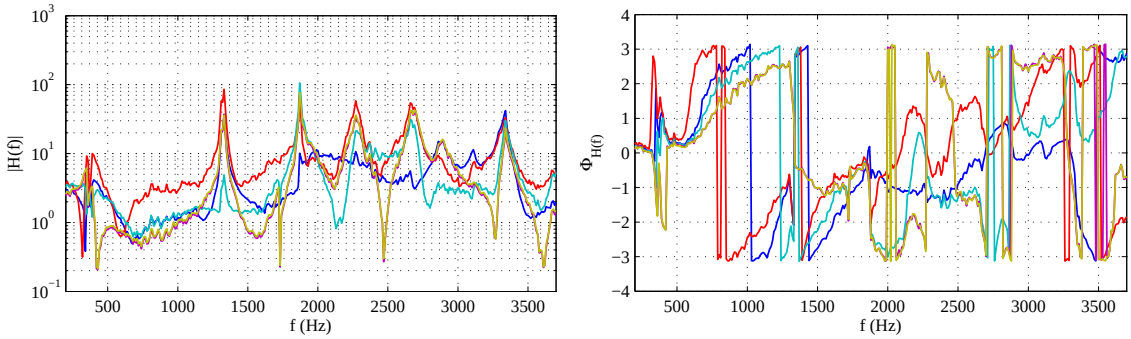

Figure 6. Module and phase of transfer functions between pressures measured at a reference microphone at the inlet of the valve and at the microphones mounted in the probe supports in the cavity. Here we excited the valve from the second supports at the bottom cavity. As one probe support is used to apply the excitation, we observe in the figure five transfer functions.

The eigenfrequencies identified here are: 1330 Hz, 1870 Hz, 2660 Hz and 3340 Hz. More frequencies were identified, for example 2270 Hz in Figure 6, but we only considered here frequencies which were excited from at least two positions of the source. The present identification is thus a first good estimation of eigenfrequencies.

The second step is to defined the mode shape with the linear acoustic solver, presented in section IV. Simulations were done for the eigenfrequencies identified experimentally. Figures 2 and 8 present the shape

of two modes respectively at 1330 and 1870 Hz. As for the experiments, these results are obtained without flow.

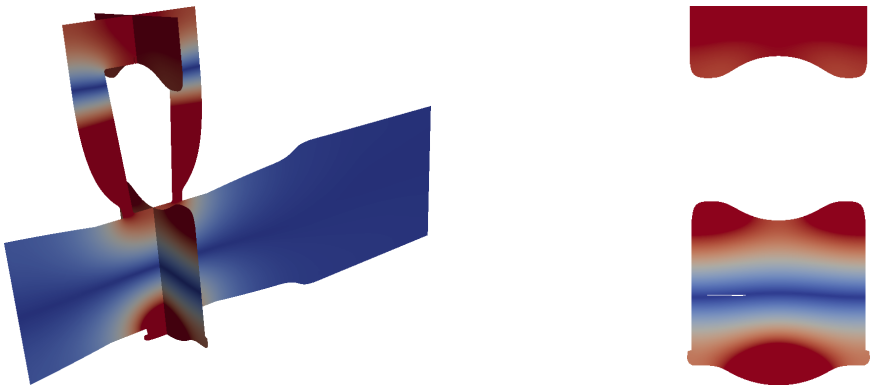

Figure 7. Visualization of the acoustic mode at a frequency $f = 1330$ Hz obtained with the linear acoustic solver. The red color stands for an extremum of the fluctuating pressure, *i.e.* a maximum of the absolute value, the blue color stands for a pressure equal to zero. On the left, a global view is depicted, on the right, we present a front cut of the valve.

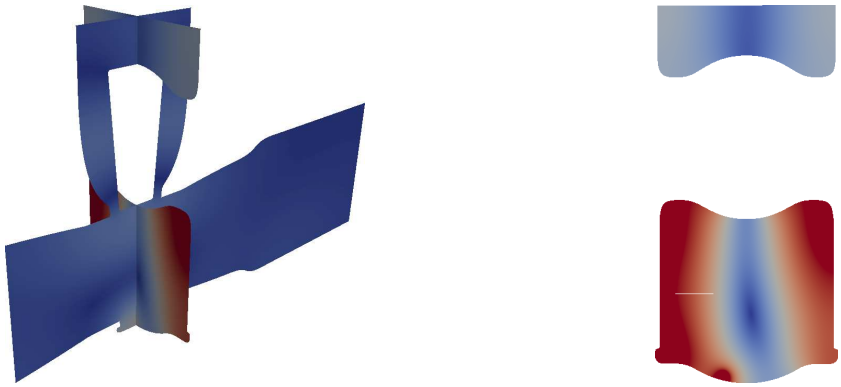

Figure 8. Visualization of the acoustic mode at a frequency $f = 1870$ Hz obtained with the linear acoustic solver. The red color stands for an extremum of the fluctuating pressure, *i.e.* a maximum of the absolute value, the blue color stands for a pressure equal to zero. On the left, a global view is depicted, on the right, we present a front cut of the valve.

For these two eigenfrequencies, we observed two different mode shapes. At 1330 Hz, the trapped mode is oriented in the height valve direction, while at 1870 Hz, the mode is oriented in the side direction. The shape of the modes, can then be compared to the phase relations between each probe measured with the experiments. By doing so, we observed a good agreement between these phase relations and the mode shape obtained with the simulations. For 1330 Hz, the pressures measured at the three bottom cavity are in-phase, and are out-of-phase with the two on the valve side. For the 1870 Hz, all the probes which are not on the center line are in-phase. The comparison of the phase relation for the probe located at the top ot the valve cavity show discrepancies between experiments and simulations. This is assumed to be acceptable for the 1870 Hz mode, as the probe is on a nodal line of the mode, but it is yet not understood for the 1330 Hz mode. For this case, further investigations are needed.

VII. Flow-acoustic results

After having characterized the acoustic eigenmodes of the valve, we focused in studying the flow-acoustic interaction over the cavity and how it generates tonal noise. This is again done by combining experiments and numerical simulations. Currently due to lack of time, experiments and simulations cannot be quantitatively compared as both do not use the same inlet flow conditions. So here we only do a qualitative comparison. In the future, hot wire measurements will be preformed and will be used as input data for the flow simulations.

Experiments

The first step thus consist of in characterizing the flow-acoustic interaction experimentally. This is done by mounting the valve model on the test rig and by measuring acoustic pressure with the six microphones for different flow velocity. The flow velocity ranges from 50 to 125 m/s with a velocity step of 2 m/s.

Figure 9 presents the evolution of the pressure level in dB as function of the frequency and the mean flow velocity above the cavity. A 3D view and a top view are represented. On this second plot, we also superimposed, with black dashed lines, the four eigenfrequencies identified with the modal analysis.

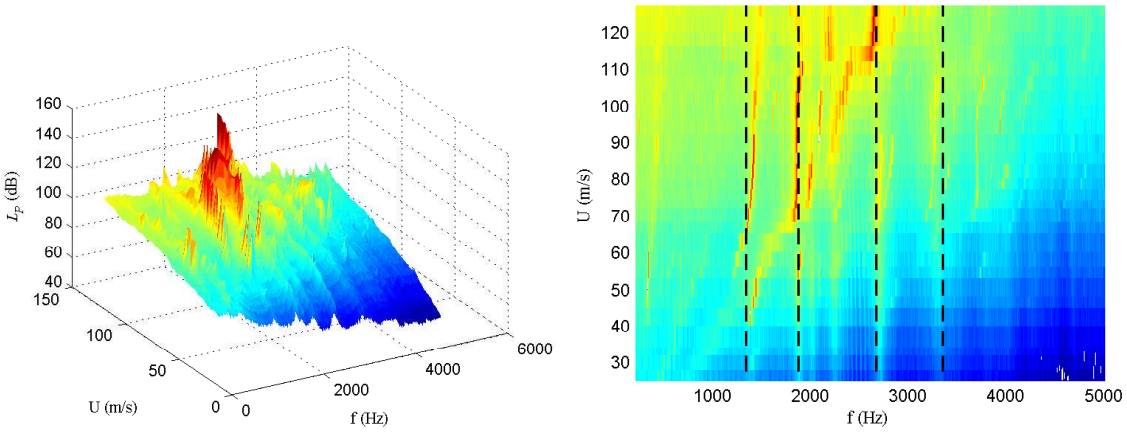

Figure 9. Pressure amplitude as a function of the frequency and the mean flow velocity above the cavity. The dashed black lines stands for the valve eigenfrequencies identified by the modal analysis without flow.

The figures show several peaks corresponding to tonal noises and the evolution of these tonal noises frequencies and amplitudes with the flow velocity. When the eigenfrequencies obtained without flow is compare to the whistling frequencies, it is observed that both are very close. Some of the whistling frequencies do not fit with the identified eigenfrequencies, but they do not correspond to the strongest tonal noise and they correspond maybe to eigenfrequencies not identified here. Indeed, we only selected eigenfrequencies which have been measured for at least two excitation at two different orifices.

Figure 10 presents in a different way the evolution of the tonal noises frequency and dimensionless acoustic pressure with the mean flow velocity above the cavity. In this figure, only the strongest tonal noise are selected. The left hand side plot present the whistling frequencies versus the flow velocity, the right hand side the dimensionless acoustic pressure versus the flow velocity. On the frequency plot, we also present the eigenfrequencies for the fluid. The dimensionless acoustic pressure is $P/(0.5\rho U^2)$, with P the acoustic pressure amplitude, ρ the fluid density and U the mean flow velocity above the cavity.

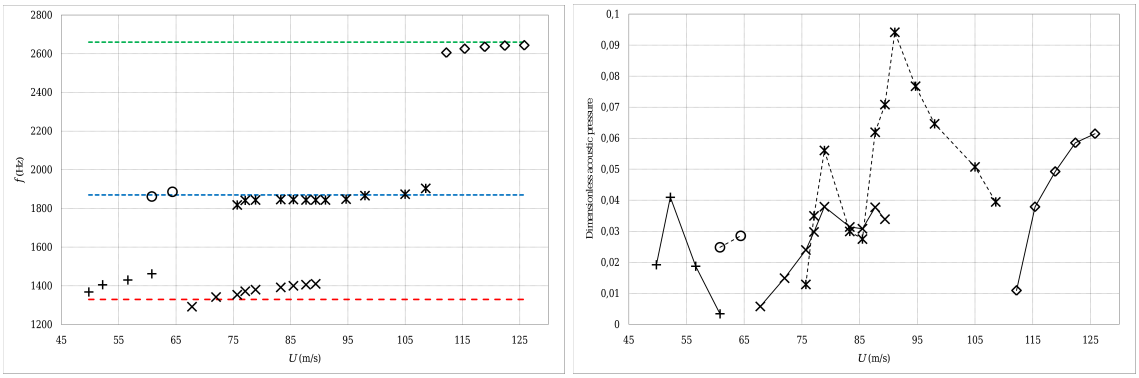

Figure 10. Evolution of the tonal noise frequency and dimensionless amplitude with the mean flow velocity above the cavity. The dashed lines in the frequency plot stands for the eigenfrequencies identified by the modal analysis. Each marker stands for a whistling at a certain acoustic mode frequency during a finite velocity flow range.

The frequency plot confirmed that the whistling frequencies coincide with the frequency of the acoustic mode of the valve. This is characteristic of self-sustained oscillations from a flow over a confined cavity.[1]

The source from the shear layer instability over the cavity is triggered by the acoustic mode of the valve. For the present case, it is observed a strong coupling between the whistling frequencies and the eigenfrequencies, as they are very close together. Moreover, this shows the slight dependence of the acoustic mode frequencies with the flow, as the tonal noise frequencies stay close to the frequencies of the acoustic mode measured with the fluid at rest.

The plot presenting the dimensionless acoustic pressure versus the mean flow velocity show that for a tonal noise triggered by the frequency of an acoustic mode, the amplitude of the tonal noise increases with the flow velocity up to a maximum and then decreases. This behavior is typical of fluid-acoustic coupling with flow over confined cavity, for which the amplitude goes up and down over each lock-in region.

Simulation

Figure 11 presents a view of the instantaneous longitudinal velocity on a streamwise section for a inlet mean flow velocity of 52 m/s. As experimental data were not available when this simulation was launched, the flow conditions are quite different between the simulation and the experiments. In the future, new simulation will be available with similar flow conditions, especially with flow profile just upstream of the cavity similar to the one measured in experiments. However, for the present case, the flow velocity visualization show the acceleration through the converging pipe, the development of a vortex over the cavity and the deceleration in the downstream diverging pipe. Downstream, we also observed the strong dissipative effect of the sponge zone. In this area the vortical structures are dissipated, with the effect of smoothing the flow velocity profile. The position of the sponge zone is based on the compromise between the length of the computational domain, strongly related to the computational time, and the proximity to the valve.

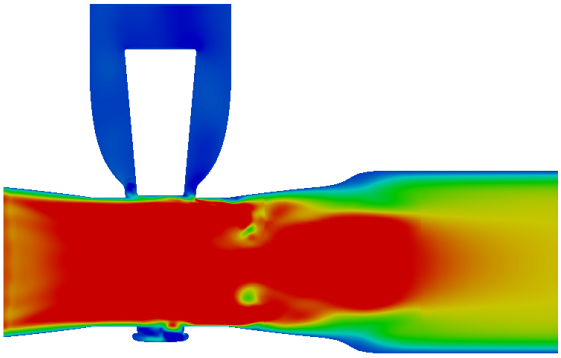

Figure 11. Gate valve flow at an inlet mean velocity of 52 m/s, that is to say a mean flow velocity just upstream of the cavity around 90 m/s. The picture gives the instantaneous longitudinal velocity on a streamwise section.

The added value of such a compressible simulation on this complex 3D geometry is to visualize the acoustic modes and the vorticity distribution to see how the shear layer modes and the acoustic modes couple together. This will be achieved in future simulations that will be performed when the experimental flow conditions will be available.

From the present simulation, acoustic pressure signal and its spectrum were calculated at the centre of the bottom cavity. These two are depicted in Figure 12. The acoustic pressure time signal exhibits an almost pure sine shape. The frequency of this sine is identified in the pressure spectrum to be equal to 1370 Hz. Comparing this frequency to the experimental results in Figure 10, there is a good agreement between experiments and numerics. Indeed the numerical frequency at 1370 Hz is very close to the experimental whistling frequency observed around 1400 Hz for a flow velocity around 90 m/s. In term of the tonal noise amplitude, the simulation gives a dimensionless acoustic pressure around 0.06. This is two times bigger than in the experiments. We consider these two values of the same order, the flow conditions being different in the experiments and the numerics.

Even if the flow conditions are different, it is observed a good agreement between experimental and numerical results for the whistling frequency and amplitude. For the rest of the acoustic spectrum, the agreement is less evident. We consider that it is due to a spectrum not yet converged, because of a too short time signal.

This preliminary result thus shows the ability of the simulation code *Code_Safari* to capture the fluid-acoustic coupling in this 3D complex geometry. The future works will consist in performing a simulation

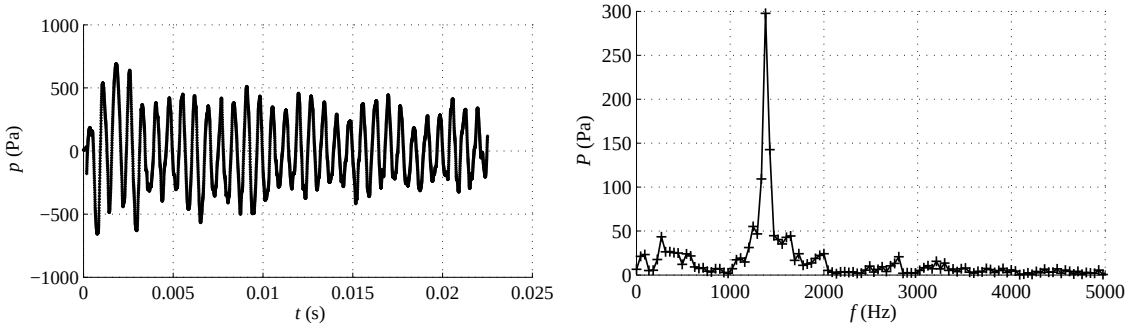

Figure 12. Pressure time signal (left) and spectrum (right) at the bottom of the cavity.

using the flow conditions measured in the experiments, particularly the inlet flow profile obtained with the hot wire probe, as input and to do a fine comparison of experimental and numerical acoustic pressure data. The simulation being validated, we may then use the simulation results to extract flow, acoustic pressure or vorticity visualization in order to characterize the free shear layer modes and the acoustic modes and how they couple together.

VIII. Conclusion

This study aims at analysing flow-acoustic interactions in an industrial gate valve. Numerical and experimental approaches are used for studying flow-acoustic phenomena in a small scale model. First an acoustic modal analysis is carried out. Experiments make it possible to identify resonance frequencies, and calculations are made with the frequency solver of *Code_Safari* in order to obtain the spatial shape of the modes. Then a flow-acoustic analysis is made. Experiments show an evolution of tonal noise in terms of frequency and amplitude with respect to the mean flow velocity that has a behaviour typical of cavity noise. The compressible LES results are in accordance with the experimental results.

A new step will be performed in the future when the measurements of flow velocity profile will be available and will help define upstream flow conditions for the flow-acoustic computations. Then experimental and numerical results will be carried in the same conditions and able for comparisons.

References

[1]K. Aly and S. Ziada. Flow excited resonance of trapped modes of ducted shallow cavities. *J. Fluids Struct.*, 26(1):92–120, 2010.

[2]K. Aly and S. Ziada. Azimuthal behaviour of flow-excited diametral modes of internal shallow cavities. *J. Sound Vib.*, 330(15):3666–3683, 2011.

[3]K. Aly and S. Ziada. Effect of mean flow on the trapped modes of internal cavities. *J. Fluids Struct.*, 33:70–84, 2012.

[4]C. Bogey and C. Bailly. A family of low dispersive and low dissipative schemes for Large Eddy Simulations and for sound propagation. *J. Comput. Phys.*, 194(1):194–214, 2004.

[5]C. Bogey and C. Bailly. Turbulence and energy budget in a self-preserving round jet: direct evaluation using large-eddy simulation. *J. Fluid Mech.*, 627:129–160, 2009.

[6]F. Daude, J. Berland, T. Emmert, P. Lafon, F. Crouzet, and C. Bailly. A high-order finite-difference algorithm for direct computation of aerodynamic sound. *Comput. Fluids*, 61:46–63, 2012.

[7]F. Daude, J. Berland, P. Lafon, F. Crouzet, C. Bailly, and W. D. Henshaw. Towards the direct computation of the aerodynamic sound generated by a gate valve in nuclear power plants. *10th Symposium on Overset Composite Grids and Solution Technology*, 2010.

[8]T. Emmert, P. Lafon, and C. Bailly. Numerical study of aeroacoustic coupling in a subsonic confined cavity. *AIAA Paper 2008-2848*, 2008.

[9]D. V. Gaitonde and M. R. Visbal. Advances in the application of high-order techniques in simulation of multi-disciplinary phenomena. *International Journal of Computational Fluid Dynamics*, 17:95–106, 2003.

[10]W. D. Henshaw. Ogen: an overlapping grid generator for Overture. Technical Report UCRL-MA-132237, Lawrence Livermore National Laboratory, 1998.

[11]V. P. Janzen, B. A. Smith, B. V. Luloff, J. Pozsgai, A. R. Dietrich, J. M. Bouvier, E. A. J., G. T. Kitko, and T. C. Roberts. Acoustic noise reduction in large-diameter steam-line gate valves. In *Proceedings of PVP 2007*, number PVP2007-26773 in ASME Pressure Vessels and Piping 2007 / Creep 8 Conference, San Antonio, Texas, 22-26$^{\text{th}}$ July, San Antonio, Texas, July 2007.

[12]P. Lafon, S. Caillaud, J.-P. Devos, and C. Lambert. Aeroacoustical coupling in a ducted shallow cavity and fluid/structure effects on a steam line. *J. Fluids Struct.*, 18(6):695–713, 2003.

[13]O. Marsden, C. Bogey, and C. Bailly. High-order curvilinear simulations of flows around non-cartesian bodies. *J. Comput. Acous.*, 13(4):732–748, 2005.

[14]D. Rockwell and E. Naudascher. Self-sustained oscillations of impinging free shear layer. *Ann. Rev. Fluid Mech.*, 11:67–94, 1979.

[15]J. E. Rossiter. Wind-tunnel experiments on the flow over rectangular cavities at subsonic and transonic speeds. *Aeronautical Research Council Reports and Memoranda*, 3438, 1964.

[16]S. E. Sherer and J. N. Scott. High-order compact finite-difference methods on general overset grids. *J. Comput. Phys.*, 210:459–496, 2005.

[17]B. A. Smith and B. V. Luloff. The effect of seat geometry on gate valve noise. *JPVT*, 122:401–407, 2000.

[18]C. K. W. Tam and Z. Dong. Radiation and outflow boundary conditions for direct computation of acoustic and flow disturbances in a nonuniform mean flow. *J. Comput. Acous.*, 4(2):175–201, 1996.

[19]M. R. Visbal and D. V. Gaitonde. On the use of higher-order finite-difference schemes on curvilinear and deforming meshes. *J. Comput. Phys.*, 181:155–185, 2002.